ICSV14
Cairns • Australia
9-12 July, 2007

USING HYSTERESIS LOOP AND TORSIONAL SHOCK LOADING TO ASSES DAMPING AND EFFICIENCY OF CYCLODRIVES

Vladis Kosse

School of Engineering Systems, Queensland University of Technology
2 George Street, GPO Box 2434, Brisbane, Australia, Q4001
v.kosse@qut.edu.au

Abstract

Cyclodrives gained popularity in the last 10...15 years. They posses many unique features such as large reduction ratio in one stage and ability to withstand up to 500% shock overloading. They are much smaller than conventional drives with a similar reduction ratio. They posses 'lost motion' up to $\pm 28^{o}$, which can be attributed to clearances and contact deformation, and it plays much greater role in Cyclodrives performance than in other kinds of drives. Despite many interesting characteristics of Cyclodrives very few research publications are available on Cyclodrive features and dynamics. In this paper a comparative analysis is conducted of Cyclodrives and other kinds of drives with very large reduction ratio in one stage. Results of experimental study of the hysteresis phenomenon in Cyclodrives and damping properties derived from dickey curves under torsional impact load are presented. The static efficiency of Cyclodrives was significantly lover of the dynamic efficiency reported by the manufacturer (in excess of 92.5%) when they are loaded up to the nominal torque, and significantly decreases when they are overloaded to 4 times the nominal torque.

1. INTRODUCTION

Cyclodrives are used in mechanical transmissions where a large reduction ratio is required. They were introduced in industrial application in the last 10...15 years [1]. The unique CYCLO operating principle was invented by the German engineer Lorenz Braren. A typical configuration of two or three cyclodisks is shown in black and white in Fig. 1. They are installed on a crankshaft and shifted apart to balance the radial load. When the crankshaft rotates, cyclodisks perform epicyclical motion and roll over the stationary rollers transmitting power to the output link – a shaft with a flange carrying rollers.

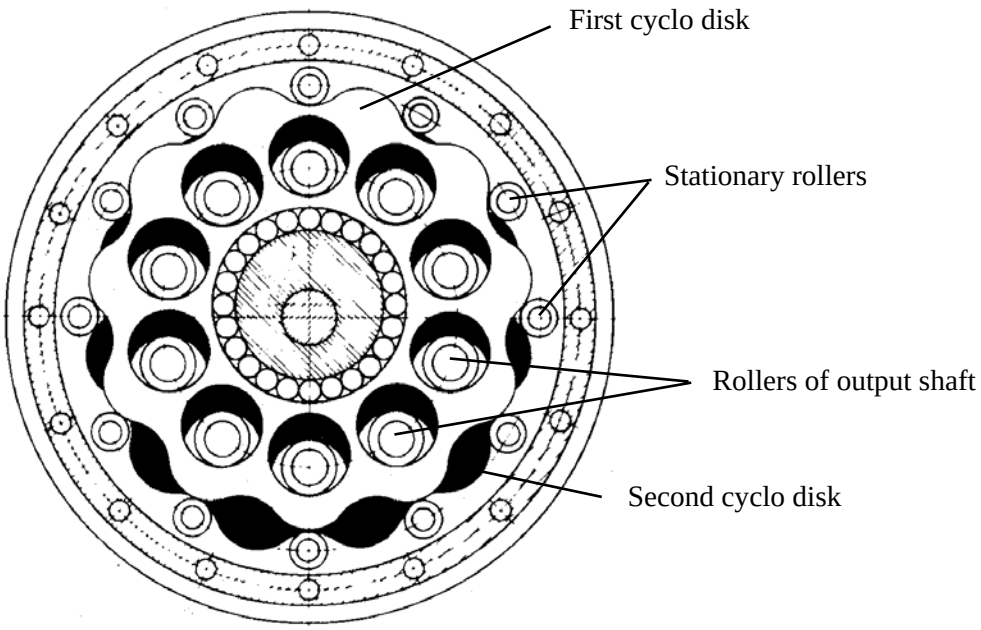

Figure 1. Schematics of Cyclodrive.

During Cyclodrive operation up to 70% of the lobes on the cyclodisks are engaged with the stationary rollers, which results in an outstanding load carrying capacity and ability to withstand shock overloading up to 500% [1]. Cyclodrives are also much smaller compared to conventional drives (by a factor of 1.5 for the same power output and reduction ratio), have high efficiency – in excess of 92.5%, suitable for frequent start-stop-reversing duties, have outstanding reliability and extended operating life – more than 20 years. Cyclodrives can provide fixed reduction ratio in one stage from 6:1 to 119:1, and up to 1,000,000:1 in triple reduction stages.

Cyclodrives possess high torsional compliance and so called 'lost motion'. If the output shaft of the Cyclodrive is locked the input shaft can be turned in both directions to an angle of up to $\pm 28^{\circ}$ under no input torque conditions [2]. When the input torque is applied the rotational displacement increases from 28° to about 50° at the nominal torque.

Comparing Cyclodrives with other drives having large reduction ratio in one stage such as epicyclic drives and harmonic drives, it can be stated that epicyclic drive also possesses 'lost motion'. However, it does not exceed 2.8° in each direction [3] and the torsional stiffness is 10 to 12 times higher than that of Cyclodrives of similar reduction ratio and power output [3]. A harmonic drive has a flexible gear (also called a flexspline) engaged with an internal rigid gear usually at two diametrally opposite sides. To provide engagement and harmonic drive operation a wave generator is inserted in the flexible gear. For small to medium size harmonic drives a wave generator with elliptic bearing is used [4], which has an elliptic inner ring and a flexible outer ring. For large harmonic drives developed for heavy machinery a disk wave generator is used [5] usually consisting off three disks mounted on a crankshaft and shifted in the opposite directions.

Inherent features of large harmonic drives are very large reduction ratio in one stage (in excess of 450:1), zero backlash, absence of 'lost motion', and large torsional compliance [5, 6, and 7]. As a result of large torsional compliance the shift in phase of up to 35° takes place between the input shaft and the tooth meshing zone. This phenomenon was initially investigated experimentally [5] and then explained theoretically [8]. It is attributed to

clearances in bearings and contact deformations in a drive train. The shift in phase phenomenon has not been observed in small harmonic drives with elliptical wave generator.

The presence of the 'lost motion' and large torsional compliance of Cyclodrives makes their drive train dynamics significantly different compared to conventional drives. Non-liner stiffness - load relationship and load-dependent damping properties make modelling of Cyclodrive dynamics very difficult. These issues have not been systematically investigated until this point in time.

2. EXPERIMENTAL INVESTIGATION OF HYSTERESIS IN CYCLODRIVES

The hysteresis phenomenon is well-known in science. A familiar example is the ferromagnetic hysteresis.

Very few attempts were made to investigate the hysteresis phenomenon in mechanical drives. Dhaouadi *et al.* [7] investigated the hysteresis phenomenon experimentally on a small harmonic drive HDC-40 from Harmonic Drive Technologies [4]. To determine the torque-displacement relationship, the output shaft of the harmonic drive was held immobile. The angular displacement was applied to the input shaft in a sinusoidal manner with controlled amplitude, and the resulting transmitted torque was measured by the torque sensor and recorded. Plotted hysteresis loops had a classical shape with loading curves for different amplitudes following the same path. The researchers acknowledge that the investigated harmonic drive demonstrated the hereditary behaviour, when the system's behaviour depends not only on the actual state of the system but on all the preceding states through which the system was passed [9]. In [7] a mathematical model of the hysteresis in harmonic drive is presented based on integro-differential equations and the hereditary concept. In this model the torque across the flexible gear is subdivided into a stiffness torque and a frictional torque taking account of the whole torque history for a given period of time. As shown in [8] in large harmonic drives, contact deformations have a heavy impact on torque-displacement diagram, thus mathematical model presented in [7] cannot be applied to harmonic drives of all sizes.

Figure 2, (a), depicts a 'classical' hysteresis curve. The Cyclodrives have a hysteresis curve split in the middle (see Figure 2, (b)) as a result of 'lost motion'. The area inside the loop represents losses in the system. If to relate this area to the area under the loading curve the efficiency of the drive can be assessed. One of the manufacturers Sumitomo Heavy Industries claims that efficiency of Cyclodrives under the nominal load is in excess of 92.5% [1]. It would be interesting to verify this value and check whether overloading affects it.

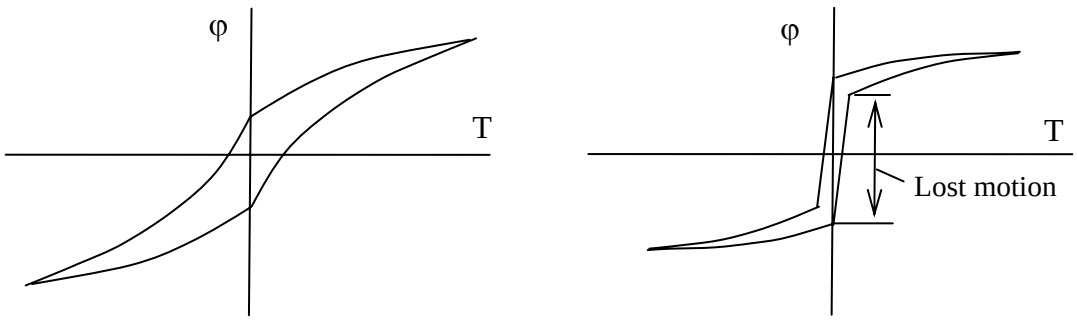

(a). Typical hysteresis loop. (b). Hysteresis loop of Cyclodrive.

Figure 2. Hysteresis loops for different drives.

2.1 Experimental setup

For an experimental investigation of the hysteresis phenomenon in Cyclodrive a special experimental setup has been developed, which is shown schematically in Figure 3. A Cyclodrive CHH-4130-87 from Sumitomo Heavy Industries (Japan) was used. It is rated for power output of **P** = 1.14 kW at the input speed of 1500 r.p.m. and the output torque of **T** = 585 Nm. The drive was placed on a rubber sheet on a bench to prevent any unwanted forces or excitations transmitted to the system from the surrounding and fixed to the bench by means of two G-clamps. The end flange of the drive was disconnected and replaced by a specially fabricated locking cup connected to the output shaft by a key joint and bolted to the housing.

To prevent the clearance in the key joint from influencing the torsional displacement, three bolts were put into the locking cup to press the key into the keyway on the output shaft. A pulley was installed on the input shaft and connected by means of a taper-lock and the key joint. Pitch radius of the pulley was **R** = 0.116 m. A circular dial with an increment of 0.5° was glued to the pulley. To take the reading of an angular displacement a pointer was fixed to the housing. To apply a couple of forces to the input shaft a synthetic rope 5 mm in diameter was wound around the pulley on the input shaft and a roller pivoted to the column attached to the Cyclodrive foot. Both ends of the rope were attached to the cross bar, and the weight hanger was attached in the middle of the cross bar.

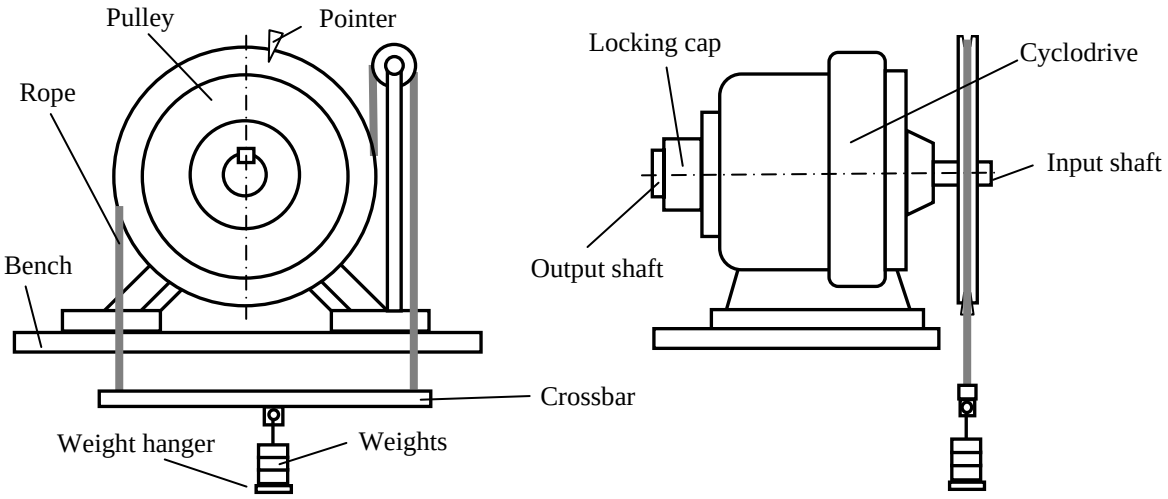

Figure 3. Experimental setup.

Weights were attached to the weight hanger with an increment of 5 N for series of experiments with the maximum input torques from $\mathbf{T_N}$ to $2\cdot\mathbf{T_N}$, and increments of 5N and 10N for series of experiments with the maximum input torques from $2\cdot\mathbf{T_N}$ to $4.5\cdot\mathbf{T_N}$ (here $\mathbf{T_N}$ is the nominal input torque). To plot a full hysteresis loop the Cyclodrive was loaded in the clock wise direction, unloaded, loaded in the counter clock wise direction and unloaded again. For each weight (and torque) increment the angular displacement was recorded, and during torque reversing the 'lost motion' was registered. Each experiment was repeated 10 times and results averaged.

The Cyclodrive was loaded to the following values of the maximum input loading torque: $\mathbf{T_N}$; $1.167\cdot\mathbf{T_N}$; $1.33\cdot\mathbf{T_N}$; and $1.5\cdot\mathbf{T_N}$, $2\cdot\mathbf{T_N}$; $2.5\cdot\mathbf{T_N}$; $3\cdot\mathbf{T_N}$; $3.5\cdot\mathbf{T_N}$; $4\cdot\mathbf{T_N}$; and $4.5\cdot\mathbf{T_N}$. For each value of the maximum loading torque the hysteresis loop was plotted.

2.2 Using Hysteresis Loop for Assessing Cyclodrive Efficiency

Figure 4 depicts hysteresis loops for values of maximum loading torque of $\mathbf{T_N}$ and $1.167 \cdot \mathbf{T_N}$.

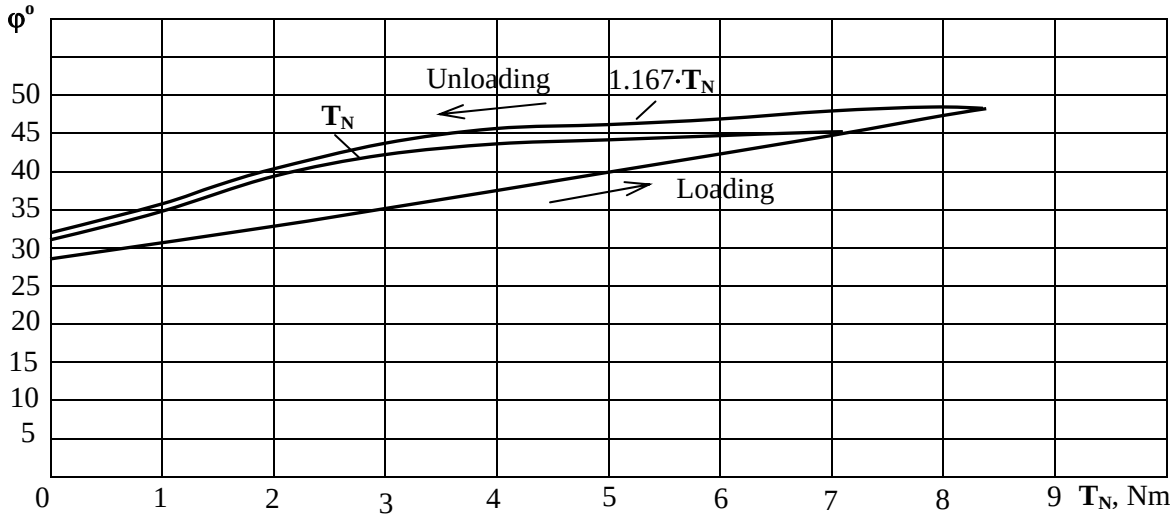

Figure 4. Hysteresis loops for $\mathbf{T_N}$ and $1.167 \cdot \mathbf{T_N}$ ($\mathbf{T_N}$ = nominal torque).

To obtain clearer picture in Fig. 4 only one half of the hysteresis loops are shown for the first quadrant. As is seen, loading curves for both values of the maximum loading torque followed the same path and were close to linear. The unloading curves followed different paths, and the hysteresis loops for smaller values of the loading torque could be fitted inside the hysteresis loop for a larger torque. It is interesting to observe that during the initial phase of unloading the hysteresis curve remained insensitive to the torque decrease and the unloading curves were almost horizontal. Only when the torque was decreased by more than 30% the angular displacement started to decrease as well.

The 'lost motion' remained ±28° in all cases, however, the width of the hysteresis loop along the vertical axis of symmetry (the difference in angular positions of the input shaft at the beginning of the loading phase and at the end of the unloading phase) increased with the value of the maximum loading torque.

The area of the loop $\mathbf{A_l}$ (area between the loading and unloading curves) represents the amount of energy lost (dissipated) in the system and to the surroundings. The area under the loading curve $\mathbf{A_o}$ (with the reference to the φ axis) represents the total energy put into the system. For the hysteresis loop corresponding to the nominal torque $\mathbf{T_N}$ these areas are: $\mathbf{A_l}$ = 5.4 square units and $\mathbf{A_o}$ = 12.5 square units respectively. The efficiency of the Cyclodrive can be assessed using a formula $\eta = ([\mathbf{A_o} - \mathbf{A_l}) / \mathbf{A_o})] \cdot 100\%$, which gives the value η = 56.8%. This value is significantly less (by a factor of 1.6) of the efficiency of Cyclodrives in excess of 92.5% reported by the manufacturer [1]. In this experiment the static efficiency was assessed (when the output shaft is fixed and the loading torque is applied to the input shaft). The manufacturer assessed dynamic efficiency when the drive train is in motion. It is well-known that static coefficient of friction is 20 to 25% greater than the dynamic coefficient of friction. Another interesting point is that when the Cyclodrive is running energy losses are associated manly with energy required to overcome rolling resistance, which is relatively small. When static efficiency is assessed energy losses are associated both with rolling resistance and deformation of the drive train elements (torsional and contact deformation), which are significantly higher than energy spent to overcome rolling resistance only.

Absence of sliding friction in Cyclodrives explains why their dynamic efficiency is significantly higher compared to other kinds of drives with similar parameters. The static efficiency of the system assessed for the maximum loading torque $2 \cdot \mathbf{T_N}$, and $4 \cdot \mathbf{T_N}$ gives values of η = 47.1%, and η = 39.68% respectively. This enables us to state that the decrease in static efficiency at $2 \cdot \mathbf{T_N}$ and $4 \cdot \mathbf{T_N}$ was by 17% and 30% respectively. This indicates that in the overloading mode the efficiency of the Cyclodrive significantly decreases.

3. USING TORSIONAL SHOCK LOADING TO ASSESS DAMPING IN CYCLODRIVE

Damping in Cyclodrives can be assessed by applying tosrional shock load and recording dickey curves. Logarithmic decrement and damping factor can be calculated by means of comparing amplitudes of neighbouring oscillation cycles [10].

3.1 Experimental Setup and Procedures

The same experimental setup was used as shown in Figure 3. Two accelerometers were attached to the pulley - one in the vicinity of the input shaft to measure radial vibrations on the shaft, and another one on the peripheral part of the pulley in the tangential direction to measure torsional vibrations. Since the excitation was applied as a couple of forces, radial vibrations of the shaft were negligible. To load the Cyclodrive to the nominal torque a mass of 6.4 kg has to be attached to the weight hanger. To apply a different torque, weights can be calculated using torques ratio. Torsional shock excitation was applied by dropping a measured weight from a specified height on the top weight attached to the weight hanger.

Experiments were conducted for different combinations of the drop weight and loading torques. In the first series of experiments a drop weight of 200 g was used and the loading torque was increased from $0.25 \cdot \mathbf{T_N}$ to $4.5 \cdot \mathbf{T_N}$ with an increment of $0.25 \cdot \mathbf{T_N}$. In the second series of experiments loading torques from $\mathbf{T_N}$ to $4 \cdot \mathbf{T_N}$ were used with an increment of $0.25 \cdot \mathbf{T_N}$, and the drop weights of 400 g and 800g.

The following instrumentation was used during experiments: eight-channel signal conditioner with amplification factor of 1, 10, and 100. The signal was supplied to two-channel oscilloscope Tektronix TDS210 through a low pass filter KH3202. The low pass filter was used to eliminate unwanted medium and high frequency signals and obtain a clear dickey curve. To transfer an image from the oscilloscope monitor to the computer screen Wave Star software was used.

3.2 Experimental Results on Torsional Impact Excitation of Cyclodrives

Figure 5 depicts dickey curves obtained for the loading torque equal to the nominal torque. Similar curves were obtained for different combinations of the loading torque and the drop weight. As is seen from Figure 5, radial vibrations of the shaft are negligible as the result of torsional excitation. The amplitude of radial vibrations is so small that the signal cannot be distinguished from the noise floor. The shape of the dickey curves for torsional vibrations indicates that the Cyclodrive is underdamped, which means the damping ratio $\varsigma < 1$ [10]. The value of the drop weight makes heavy impact on the shape of the dickey curves. Larger values of the drop weight decrease the natural frequency and increase the time required to damp vibrations. The logarithmic decrement δ can be found using the following expression [10]

$$\delta = (1 / n) \cdot \mathbf{ln}(X_{\mathbf{o}} / X_{\mathbf{n+1}}), \quad (1)$$

Where, n = cycle number; $X_{\mathbf{i}}$ = amplitude corresponding to the **i**-th cycle.

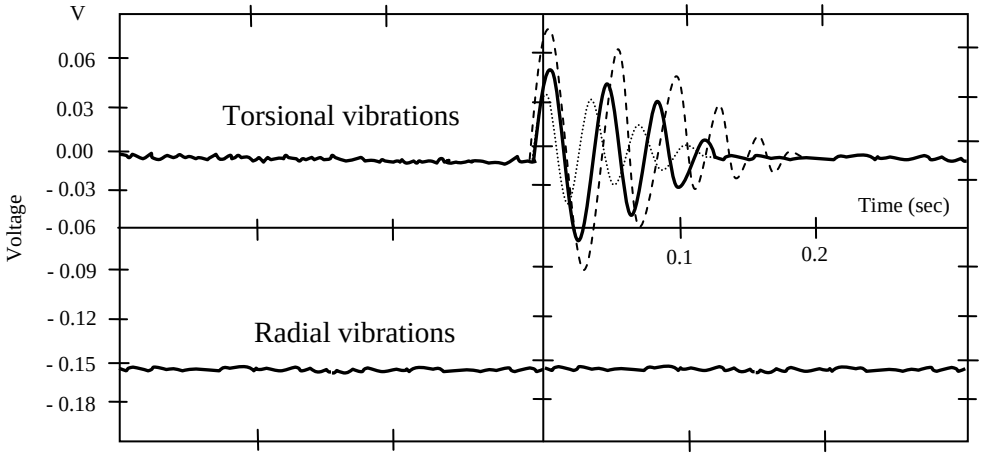

Figure 5. Dickey curves recorded for the loading torque equal to the nominal torque $\mathbf{T_N}$ and different drop weights (---- 800g; —— 400g; ····· 200g). Upper curves represent torsional vibrations, lover curve - radial vibrations of the input shaft.

For the known value of the logarithmic decrement the damping ratio can be found as follows,

$$\varsigma = \delta / \sqrt{(2\pi)^2 + \delta)}. \quad (2)$$

Values of the logarithmic decrement and damping ratio calculated using expressions (1, 2) for the nominal loading torque and different values of the drop weight are shown in Table 1.

Table 1. Values of the logarithmic decrement δ and damping ratio ς

Loading torque	Drop weights, **g**	Logarithmic decrement, δ	Damping ratio, ς
$\mathbf{T_N}$	200	1.053	0.1652
	400	0.787	0.1243
	800	0.443	0.0703

As is seen from the Table 1 heavier excitation with larger drop weights results in less effective damping. Torsional shock loading with the drop weight of 200 g results in the damping ratio more than two times greater than that for the drop weight of 800 g. The natural frequency of torsional vibrations **f** (Hz) under the nominal torque $\mathbf{T_N}$, decreased from 25.6 Hz for the drop weight of 200 g, to 20.45 Hz for the drop weight of 800 g, which indicates that heavier shock load generates free vibrations at a lower frequency. Time response is also different. For small shock excitation vibrations die quicker (see also Figure 5).

4. CONCLUSIONS

In this paper results of a systematic experimental research on static efficiency and damping properties of Cyclodrives are presented. Main findings can be summarised as follows.

- The ‘lost motion’ and high torsional compliance in Cyclodrives play much greater role than in other types of drives.
- The static efficiency of the Cyclodrive when it is loaded up to the nominal torque is by a factor of 1.6 times smaller than dynamic efficiency reported by the manufacturer.
- The static efficiency of the Cyclodrive decreases by 17% when it is overloaded to twice the loading torque. Further overloading up to four times the nominal torque causes decrease by 30%.
- Significantly higher dynamic efficiency of Cyclodrive can be attributed to the factor that in a running Cyclodrive energy losses are associated with rolling resistance only, and dynamic coefficient of friction is significantly smaller that static coefficient of friction.
- When the Cyclodrive is fully loaded or overloaded small variations in the loading torque do not cause any notable change in the angular displacement of the shaft.
- Heavier excitation with large drop weights results in less effective damping.
- Torsional shock loading with the drop weight of 200 g results in the damping ratio more than two times greater than that for the drop weight of 800 g.
- The natural frequency of torsional vibrations under the nominal torque $\mathbf{T_N}$, decreases with the increase of the drop weight, which indicates that heavier shock load generates free vibrations at a lower frequency.
- For small shock excitation vibrations die quicker.

REFERENCES

[1] *Speed Reducers and Gear Motors*, Catalogue No. 990341, Sumitomo Heavy Industries Cyclo Drive (Europe) GmbH.

[2] V.Kosse, Experimental investigation of torsional stiffness of mechanical drives with large reduction ratio, Part 1: Cyclodrives. *Proceedings of the 10-th Asia-Pacific Vibration Conference*, 12-14 November 2003, Royal Pines Resort, Gold Coast, Australia.

[3] V.Kosse, Experimental investigation of torsional stiffness of mechanical drives with large reduction ratio, Part 2: Epicyclic drives. *Proceedings of the 10-th Asia-Pacific Vibration Conference*, 12-14 November 2003, Royal Pines Resort, Gold Coast, Australia.

[4] *HDC Cup Component Gear Set Selection Guide*, Harmonic Drive Technologies, Peabody, MA, 1995.

[5] V.Kosse and M.Margulis, *Design, manufacture and investigation of power transmissions for metallurgical converters and mixers incorporating harmonic drives*, UkrVINITI, Mariupol, No. 97UK86, Ukraine, 1986.

[6] V.Kosse and M.Margulis, Analytical determination of torsional stiffness of a high-torque harmonic drive. In a book: *Advanced Technology in Machine Building Industry*, USSR, Kramatorsk, NIIPTMASH, 1986.

[7] R.Dhaouadi, F.H.Ghorbel, and P.S.Gandhi, A new dynamic model of hysteresis in harmonic drives. IEEE Transactions on Industrial electronics, **Vol. 50**, No. 6 (2003).

[8] V.Kosse, Analytical investigation of the change in phase angle between the wave generator and the teeth meshing zone in high torque mechanical harmonic drive. *Mechanism and Machine Theory*, **32** (5) (1997) 533-538.

[9] E.Volterra. Vibration of elastic systems having hereditary characteristics. *Journal of Applied Mechanics*, Vol. **17**, Dec. 1950, pp. 363-371.

[10] Robert F. Steidel, *An Introduction to Mechanical Vibrations*, Third edition, John Willey & Sons, Inc. 1989.